

Nonlinear Radiation Pressure and Stochasticity in Ultraintense Laser Fields

Joel E. Moore

Department of Physics, Massachusetts Institute of Technology, Cambridge, MA 02139

(February 13, 1998)

The drift acceleration due to radiation reaction for a single electron in an ultraintense plane wave ($a = eE/mc\omega \sim 1$) of arbitrary waveform and polarization is calculated and shown to be proportional to a^3 in the high- a limit. The cyclotron motion of an electron in a constant magnetic field and an ultraintense plane wave is numerically found to be quasiperiodic even in the high- a limit if the magnetic field is not too strong, as suggested by previous analytical work. A strong magnetic field causes highly chaotic electron motion and the boundary of the highly chaotic region of parameter space is determined numerically and shown to agree with analytical predictions.

PACS numbers: 52.40.Nk 52.35.Mw

It has been known for many years that qualitative changes occur in the behavior of an electron moving in an electromagnetic plane wave when the dimensionless strength $a = eE/mc\omega$ is of order unity. Recent advances in laser pulse compression and amplification [1] have made it possible to attain such ultraintense waves in the laboratory and led to new investigations of their properties. One important effect is that an electron moving in an ultraintense electromagnetic plane wave and also subjected to slowly varying “background” fields behaves approximately like a particle of enhanced mass $m\gamma_0 = m\sqrt{1 + e^2\langle A_\mu A^\mu \rangle}/m^2c^4$ drifting in the background fields. Here A is the vector potential and $\gamma_0 = \sqrt{1 + a^2/2}$ for a linearly polarized monochromatic wave. The fast motion in the wave can be rigorously averaged over if the background fields are sufficiently weak and the plane wave is not so strong that pair creation effects become significant.

The first part of this Letter uses the guiding-center equations obtained in the derivation of the enhanced-mass approximation [2] to calculate the drift acceleration of an electron in a plane wave due to the radiation damping and reaction forces. In a strong wave, the variation of the electron effective mass $m\gamma$ over the wave orbit must be properly accounted for to obtain the correct drift acceleration. The average drift acceleration is the quantity of greatest interest because experiments and astrophysical phenomena typically involve many wave periods. The guiding-center equations provide the tools to carry out the averaging and determine the motion of electrons under the (previously calculated) Lorentz-Dirac radiation force [3,4]. The second part of this Letter considers the destruction of the enhanced-mass behavior and transition to stochasticity as the strength of the background fields is increased to violate the field-strength condition $eB_{\text{back}}/mc\omega_{\text{wave}} \ll 1$ necessary for the enhanced-mass derivation. The breakdown of the enhanced-mass picture is shown numerically to predict the onset of stochasticity even for very strong wave intensity. Both the nonlinear radiation acceleration and the stochasticity are expected

to be significant in astrophysical situations, and the first effect may well be visible in laboratory experiments with ultraintense laser pulses.

Classical calculations are valid for high a as long as the discrete photon energy $\hbar\omega \ll mc^2$ and the amplitude for QED processes such as e^+e^- pair creation is small ($eE\hbar/mc \ll mc^2$) [5]. The classical high- a regime includes a number of existing and proposed accelerator designs, such as the plasma wakefield and beat-wave accelerators [6]. Lasers used in the National Ignition Facility and similar inertial fusion projects have $a \sim 1$ so strong-field effects are significant. Many astrophysical problems also involve high- a radiation sources, and in particular consequences of strong-wave radiation damping are discussed in [7].

The motion of an electron in a plane wave of arbitrary intensity is integrable both classically and within the Dirac equation. This occurs because a third conserved quantity $\gamma - p_x$ exists in addition to the two transverse generalized momenta. Here γ is the electron Lorentz factor and p_x is the component of electron momentum along the wave axis. Including radiative effects or adding additional fields generally violates this conservation. The result of the scattering of the wave by the electron is a force on the electron along the wave axis, which has the form $F = 2e^4\langle \mathbf{E}^2 \rangle/3m^2c^4$ for weak plane waves. In the high- a regime the electron radiates much more strongly ($\propto a^4$ rather than a^2 in the low- a limit) and radiates high harmonics of the wave frequency [3,4].

Previous work on the motion caused by radiation reaction in a strong wave has included numerical studies [8,5] and solutions to the Lorentz-Dirac equation (in the Landau approximation [3]) in special cases such as monochromatic linearly and circularly polarized waves [9]. The guiding-center formalism gives a simple result for the drift velocity, the quantity of primary interest, valid for an arbitrarily polarized, polychromatic wave. The two approximations involved are the Landau approximation that the radiation force is calculated from the trajectory in the absence of the radiation force, and the guiding-

center approximation that the changes in the drift velocity over a single orbit are nonrelativistic and hence add linearly, which is well satisfied for radiation reaction in the classical regime. An additional advantage of the guiding-center formalism is that multiple applied forces effectively superpose, which is not in general the case for nonlinear equations of motion.

The motion in a wave along $\hat{\mathbf{x}}$ with dimensionless vector potential $\mathbf{A}(t - x/c) = \mathbf{A}(\eta)$ is given in the “drift frame” where the electron has zero average velocity by $p_i = -mcA_i$ for the transverse components, and $p_x = mc(\mathbf{A}^2 - \langle \mathbf{A}^2 \rangle)/2\gamma_0$, with $\langle \rangle$ indicating averaging over η and $\gamma_0^2 = 1 + \langle \mathbf{A}^2 \rangle$. The wave envelope is assumed constant in η so that the averages are well-defined. Variation in the wave envelope causes a ponderomotive force, reviewed below.

The radiation reaction force from scattered photons causes the drift velocity (the velocity of the drift frame) to change in time. The drift velocity component along the wave axis changes for an applied force \mathbf{F} (in addition to the force from the wave) according to [2]

$$\frac{dv_d^x}{dt} = \frac{F_x}{m\gamma} - \frac{F_y v_y}{mc\gamma_0} - \frac{F_z v_z}{mc\gamma_0}. \quad (1)$$

Note that the instantaneous drift acceleration from an applied force is not necessarily in the direction of the applied force. The causality problems with the Lorentz-Dirac classical radiation force [5] do not appear in the Landau approximation, which is valid if the radiation force is a small perturbation on the motion causing the radiation. The instantaneous radiation force on the electron is

$$\begin{aligned} F_i &= \frac{2e^2}{3mc^3} \left[\frac{d}{dt} (\gamma \frac{dp_i}{dt}) - \frac{v_i \gamma^2}{mc^2} \left(\left(\frac{d\mathbf{p}}{dt} \right)^2 - \left(\frac{dE}{cdt} \right)^2 \right) \right] \\ &= \frac{2e^2 \gamma_0^2}{3mc^3} \left[\frac{d^2 p_i}{d\eta^2} - \frac{v_i \gamma_0^2}{mc^2} \left(\left(\frac{d\mathbf{p}}{d\eta} \right)^2 - \left(\frac{dE}{cd\eta} \right)^2 \right) \right]. \end{aligned} \quad (2)$$

Upon substituting (2) into (1), we obtain the instantaneous acceleration (w.r.t. phase) in the x-direction: $dv_d^x/d\eta = 2e^2\gamma_0(d\mathbf{A}/d\eta)^2/3mc^2$. Now the averaging over η is simple. For a wave with intensity per frequency interval $I(\omega)$, the result is

$$\left\langle \frac{dv_d^x}{dt} \right\rangle = \frac{8\pi e^4}{3m^3 c^5} \int I(\omega) d\omega \sqrt{1 + \frac{4\pi e^2}{m^2 c^3} \int \frac{I(\omega) d\omega}{\omega^2}}. \quad (3)$$

The acceleration is thus independent of polarization and the phasing between different frequencies, just as in the nonrelativistic limit, but scales with a^3 rather than a^2 for large a .

For a linearly polarized monochromatic wave, the average acceleration is $2e^2\omega^2(a^2/2 + a^2/4)\sqrt{1 + a^2/2}/3mc^2$. For circular polarization, the result is $2e^2\omega^2(a^2 + a^4)\sqrt{1 + a^2}/3mc^2$. These are essentially identical to the considerably less transparent solutions in [9]. For circular polarization this is just the radiated power divided

by $\bar{m}c$, with $\bar{m} = m\gamma_0$. For linear polarization this is not the case, but the correct acceleration is obtained if we account for the fact that the electron’s total radiated momentum is nonzero, unlike for circular polarization [4]. The correct average radiation acceleration is thus obtained from conservation of energy and momentum *if* a drifting electron is assigned momentum $m\gamma_0 v_d$. However, there is no *a priori* reason for this assignment without the use of (1).

The average radiation force can be defined as the required constant force to balance the above acceleration: $F_{\text{rad}} = m\gamma_0 A_{\text{rad}}$. The radiation force from a blackbody source of intensity I and temperature T is

$$F_{\text{rad}} = \frac{8\pi e^4 I}{3m^2 c^5} \left(1 + \frac{10\hbar^2 e^2 I}{\pi m^2 c^3 k_B^2 T^2} \right). \quad (4)$$

Changes in the envelope of a plane wave cause a ponderomotive force, which conserves $\gamma - p_x$ is directed forward when the wave is rising and backward when the wave is falling. (There are also transverse ponderomotive forces in real beams arising from the finite spot size; these have a different character and are not discussed here.) The radiation force does not conserve $\gamma - p_x$ and always acts in the forward direction. Treating an electron in a plane wave as an enhanced-mass particle acted upon by ponderomotive and radiation forces gives a simple and accurate description of single-particle behavior in the classical regime.

Now we turn to consider the second problem mentioned in the opening: the destruction of the enhanced-mass picture when strong constant electromagnetic fields are added to the plane wave. It will be shown that for one typical field configuration, i.e., one without special symmetries giving rise to integrability, the breakdown of the enhanced-mass picture is consistent with the analytical predictions of [2] and associated with the onset of stochasticity over a wide range of beam intensity. An example of an integrable configuration is an applied magnetic field parallel to the wave axis [10]. In the following the wave will be taken to have constant amplitude and the radiation force will be neglected. We study a constant magnetic field $\mathbf{B} = B\hat{\mathbf{z}}$ perpendicular to a linearly polarized wave $A_y(\xi)$ traveling in the $\hat{\mathbf{x}}$ direction. Then p_z is constant and we take $p_z = 0$ so that the electron motion is confined to the xy plane. For small wave strength $a_w = eE/mc\omega$ the motion can be analyzed perturbatively because the equations of motion are nearly linear [11].

When a_w is of order unity, the equations are strongly nonlinear and new phenomena appear. However, the motion is still simple for $a_w > 1$ as long as the applied magnetic field is not too strong. In the derivation of the equations for the motion of the guiding-center, it was necessary to assume $a_b = eB/mc\omega = \omega_c/\omega \ll 1$, i.e., the electron is far from resonance. Fig. 1 shows a typical trajectory in the enhanced-mass regime: the electron

executes fast oscillations in the wave, while its guiding-center makes a slow orbit in the magnetic field. The relativistic nonlinearity in the equations of motion can destroy quasiperiodicity, but only for $\omega_c/\omega \sim 1$.

With no wave present the gyrocenter of the electron motion $(x_0, y_0) = (x + p_y/eB, y - p_x/eB)$ (with $m = c = 1$) is constant in time. The electron still has an exactly constant gyrocenter for an arbitrarily strong wave:

$$(K_x, K_y) = \left(x + \frac{p_y + eA_y(\xi)}{eB}, y - \frac{p_x + 1 - \gamma}{eB}\right). \quad (5)$$

Such a gyrocenter exists for any direction of the magnetic field $B_0 \hat{\mathbf{b}}$ and any polarization of the wave: $\mathbf{r}_c = \mathbf{r} - (\mathbf{r} \cdot \hat{\mathbf{b}})\hat{\mathbf{b}} - \hat{\mathbf{b}} \times (\mathbf{p} + e\mathbf{A}(\xi) + 1 - \gamma\hat{\mathbf{k}})/eB_0$.

Now consider again the particular case $\hat{\mathbf{k}} \parallel \hat{\mathbf{x}}$, $\mathbf{A} \parallel \hat{\mathbf{y}}$, $\mathbf{B} \parallel \hat{\mathbf{z}}$. Taking $p_z = 0$ confines the motion to the xy plane so that phase space is five-dimensional (position (x, y) , momentum (p_x, p_y) , and time t). The constants (5) reduce the effective dimension of phase space by two. Choosing particular values $K_x = K_y = 0$ of the constants corresponds to shifting the gyrocenters of all possible trajectories to the origin, removing two translational degrees of freedom. After this shift, p_x and p_y are no longer independent coordinates but rather functions of x and y determined by (5).

The existence of two constants of motion reduces the effective phase space in this particular case from five dimensions to three. Hamiltonian motion in a two-dimensional phase space is always integrable, so that three-dimensional motions such as the driven pendulum and the Chirikov-Taylor problem [12] are the simplest that can exhibit nonintegrable behavior. The equations of motion after a change to the independent variable $\eta = t - x/c$ and introducing dimensionless parameters $a_b = \omega_c/\omega$, $a_w = eE_0/mc\omega$, and a monochromatic wave $A(\eta)$ are ($\omega = m = c = 1$):

$$\begin{aligned} \gamma &= 1 + \frac{a_b^2 y^2 + (a_b x - a_w \sin \eta)^2}{2(1 + a_b y)} \\ \frac{dx}{d\eta} &= \frac{\gamma}{1 + a_b y} - 1, \quad \frac{dy}{d\eta} = \frac{a_b x - a_w \sin \eta}{1 + a_b y}. \end{aligned} \quad (6)$$

These equations are integrated numerically for various values of a_b , a_w , and the initial conditions $x(\eta_0), y(\eta_0)$.

The equations of motion (6) are periodic in η and plotting the electron's (x, y) coordinates after each period gives an area-preserving map of the plane to itself. Fig. 2 shows trajectories under this map. For low values of the electron initial energy, the motion is quasiperiodic and nearly circular, while for large values of the initial energy the motion is chaotic, as demonstrated by numerically calculated Liapunov exponents (Fig. 3). As time increases the largest exponent for trajectories beginning on points D, E, F remains positive, indicating that neighboring initial points separate exponentially rapidly [13]. The electron's initial energy affects the character of the

motion because a_b can be much larger in the rest frame of an electron than in the lab frame if the electron has a large initial velocity. To eliminate this effect the initial electron drift velocity is fixed at $0.5c$ henceforth.

The enhanced-mass description predicts that the guiding-center of the electron moves in a circle: $(x_{\text{gc}}(t), y_{\text{gc}}(t)) = (x_0 + (v_d/\Omega) \sin \Omega t, y_0 + (v_d/\Omega) \cos \Omega t)$, with $v_d = 0.5c$ and $\Omega = \omega_c/\gamma_0\gamma_d = a_b\omega\sqrt{1 - v_d^2}/\gamma_0$. At the end of each wave period, $x_{\text{gc}}(t)$ and $y_{\text{gc}}(t)$ are compared with the actual location of the guiding-center calculated from (6). As a dimensionless error measure we use the normalized sum of squares error over a cyclotron orbit: $E_{\text{gc}} = (\Omega/v_d)^2 \sum (\mathbf{r}(t) - \mathbf{r}_{\text{gc}}(t))^2$. The error is found to be quite small ($E_{\text{gc}} < 0.01$) for all values of a_w studied as long as $a_b < 0.04$. For each value of a_w , E_{gc} increases rapidly to order unity once a_b reaches a certain critical field: as a threshold we define $a_b^{\text{crit}}(a_w)$ as the value of a_b where $E_{\text{gc}} = 0.01$. Consistent with the predictions of the enhanced-mass picture, a_b^{crit} remains nonzero for large a_w and in fact increases slightly with a_w . Even though high a_w makes the equations (6) quite nonlinear, the motion remains quasiperiodic and nearly circular for $a_b < a_b^{\text{crit}}$.

As a_b increases above a_b^{crit} , the trajectory with initial velocity $0.5c$ becomes chaotic (has a positive Liapunov exponent) at some value a_b^* . For large a_w , above a_b^* the motion is strongly chaotic and the electron energy fluctuates wildly. This differs from nearly linear resonance at small a_w in that no tuning of frequencies is necessary for energy gain and hence energy gain is not limited by relativistic detuning. Fig. 4 shows numerical curves for a_b^{crit} and a_b^* as part of a schematic phase diagram. The two curves are adjacent over four decades of beam intensity. The dotted line (which was not calculated and is only schematic) separating the quasilinear resonance phase from the strong stochasticity phase can be defined by the destruction of the last invariant torus at large energy, since in three dimensions such a torus bounds the energy of trajectories contained within it. Rax has previously proposed that the stochastic motion of electrons in *multiple* plane waves may give rise to high-energy cosmic rays [14]. The considerations above indicate that a single plane wave, together with a sufficiently strong magnetic field, is sufficient.

We verified that approximately the same boundary for the guiding-center description applies when the wave contains two or three frequencies. It seems natural to conjecture that the guiding-center region in Fig. 4 also describes waves of finite bandwidth and other orientations of the magnetic field (excluding the integrable case $\mathbf{B} \parallel \mathbf{k}$).

The author wishes to thank Deepak Dhar for many helpful conversations. This work was supported by a U.S. Fulbright grant and a fellowship from the Hertz Foundation.

-
- [1] M. D. Perry and G. Mourou, *Science* **264**, 917 (1994).
 - [2] J. E. Moore and N. J. Fisch, *Phys. of Plasmas* **1**, 1105 (1994).
 - [3] L. D. Landau and E. M. Lifshitz, *The Classical Theory of Fields*, 4th revised English ed. (Pergamon, London, 1975), §48, 73, 78.
 - [4] E. S. Sarachik and G. T. Schappert, *Phys. Rev. D* **1**, 2738 (1970).
 - [5] F. V. Hartemann and A. K. Kerman, *Phys. Rev. Lett.* **76**, 624 (1996).
 - [6] T. Tajima and J. M. Dawson, *Phys. Rev. Lett.* **43**, 267 (1979); P. Chen and J. M. Dawson, in *Laser Acceleration of Particles*, ed. C. Joshi and T. Katsouleas, AIP Conf. Proc. No. 130 (American Institute of Physics, New York, 1985).
 - [7] W. H. Kegel, H. Herold, H. Ruder, and R. Leinemann, *Astron. and Astrophys.* **297**, 369 (1995).
 - [8] M. Grewing and H. Heintzmann, *Phys. Rev. Lett.* **28**, 381 (1972).
 - [9] K. Anders, Staatsexamensarbeit, Universitat Kiel, 1987.
 - [10] C. S. Roberts and S. J. Buchsbaum, *Bull. Am. Phys. Soc.* **9**, 14 (1964).
 - [11] C. F. F. Karney, *Phys. Fluids* **21**, 1584 (1978).
 - [12] B. V. Chirikov, *Phys. Rep.* **52**, 265 (1979).
 - [13] A. J. Lichtenberg and M. A. Lieberman, *Regular and Chaotic Dynamics*, 2nd edition (Springer-Verlag, New York, 1992), p. 298.
 - [14] J.-M. Rax, *Phys. Fluids B* **4**, 3962 (1992).

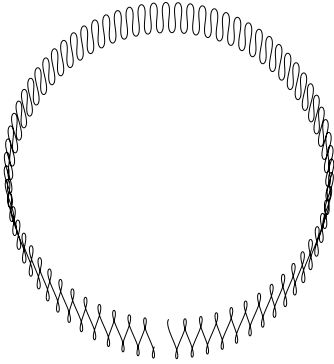


FIG. 1. Typical electron cyclotron motion with $a_w = 1.5$, $a_b = 0.02$, $\mathbf{B} \parallel \hat{\mathbf{z}}$ and $\mathbf{k} \parallel \hat{\mathbf{x}}$.

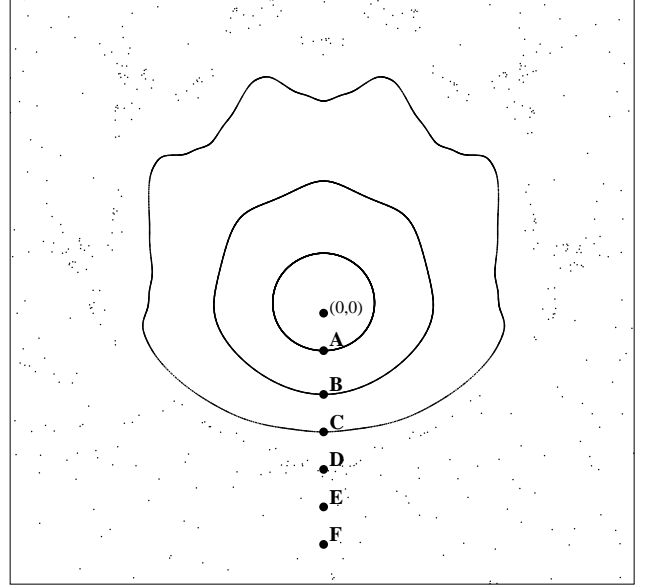


FIG. 2. Surface of section showing trajectories from six different initial conditions with $a_w = 0.1$, $a_b = 0.18$.

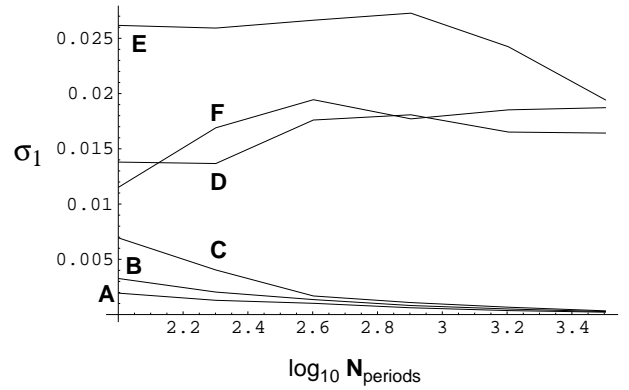


FIG. 3. Numerical largest Liapunov exponent σ_1 calculated at different times for trajectories starting on the six labeled points in Fig. 2.

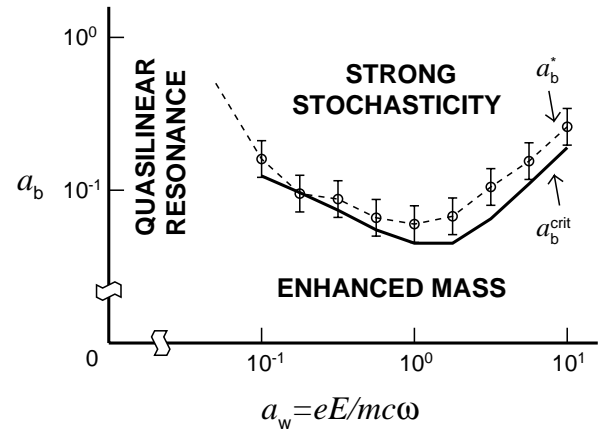


FIG. 4. Numerical values a_b^{crit} and a_b^* for various a_w as part of schematic phase diagram. Error bars are shown for a_b^* because it is difficult to determine precisely when the largest Liapunov exponent becomes positive.